Journal of
Applied Crystallography
ISSN 0021-8898
Editor: **Anke R. Pyzalla**

Flat-plate single-crystal silicon sample holders for neutron powder diffraction studies of highly absorbing gadolinium compounds

D. H. Ryan and L. M. D. Cranswick

J. Appl. Cryst. (2008). **41**, 198–205

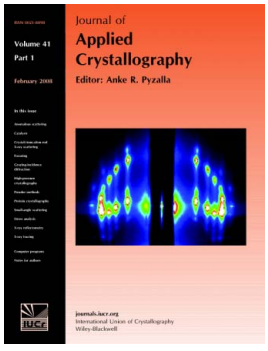

Journal of
Applied Crystallography
ISSN 0021-8898

Received 11 September 2007
Accepted 5 December 2007

Flat-plate single-crystal silicon sample holders for neutron powder diffraction studies of highly absorbing gadolinium compounds

D. H. Ryan[a] and L. M. D. Cranswick[b]*

[a]Physics Department and the Centre for the Physics of Materials, McGill University, 3600 University Street, Montreal, Quebec, Canada H3A 2T8, and [b]Canadian Neutron Beam Centre, National Research Council of Canada, Building 459, Station 18, Chalk River Laboratories, Chalk River, Ontario, Canada K0J 1J0. Correspondence e-mail: lachlan.cranswick@nrc.gc.ca

The extreme absorption cross section of natural gadolinium has so far precluded routine neutron diffraction work on its alloys and compounds. However, it is shown here that an easily constructed flat-plate sample holder with silicon single-crystal windows can be used to place a thin layer of material in a neutron beam and obtain Rietveld refinement quality diffraction data in a modest time. The flat-plate geometry uses a large area to compensate for the necessarily thin sample. Demonstration data are presented on two intermetallic compounds, $Sm_3Ag_4Sn_4$ and $Gd_3Ag_4Sn_4$, and it is shown that both structural and magnetic information can be derived from the diffraction patterns. By working at a wavelength of 2.37 Å, it is possible to observe the low-Q diffraction peaks associated with magnetic ordering. This simple methodology should now enable routine measurements on even the most highly absorbing materials.

1. Introduction

Neutron diffraction is, without doubt, the most important technique for studying magnetic order, but many of the rare earths exhibit significant absorption, making their use in diffraction experiments difficult. At a thermal neutron wavelength of 1.80 Å, absorption (Rauch & Waschkowski, 2003) by dysprosium [σ_{abs} = 994 (13) b; 1 b = 10^{-24} cm^2] is problematic, and both europium [4530 (40) b] and samarium [5922 (56) b] present serious challenges. However, the extreme absorption cross section of natural gadolinium [49 700 (125) b, the largest of any element] makes it more suitable for neutron shielding than neutron diffraction. Indeed, metallic gadolinium has an absorption length of only 7 µm, making it an order of magnitude better for shielding than the more conventional cadmium metal. Despite the extreme problems gadolinium presents, the importance of understanding the magnetic behaviour of its many remarkable compounds has led us to seek ways of carrying out powder diffraction measurements on gadolinium-based materials.

In a recent paper (Potter *et al.*, 2007), two low-background sample holders based on inexpensive single-crystal silicon were described. One single-crystal silicon sample holder used a conventional cylindrical geometry and was optimized for weakly scattering materials. The other used a large-area flat-plate geometry and was designed for working with highly absorbing samples, the original focus being Eu_2BaNiO_5. Both holders yielded much lower backgrounds than more conventional null-matrix or null-scattering materials and were essentially free from interfering Bragg peaks.

We show here that the large-area flat-plate holder can be used for samples that have even higher neutron absorption cross sections than the Eu_2BaNiO_5 compound used in the developmental study, and demonstrate its use for compounds of samarium and gadolinium. The construction of the sample holder was described in detail in our earlier paper (Potter *et al.*, 2007) and so we will only cover its use and evaluation here. All the following powder diffraction data were collected using the C2 powder neutron diffractometer at Chalk River, the system details of which are described by Potter *et al.* (2007).

2. Overview of neutron diffraction of gadolinium compounds

Gadolinium is, in principle, the simplest of the magnetic rare earths, as its half-filled 4*f* shell gives it a spherical (L = 0) ground state with, nominally, zero orbital moment. With the major source of anisotropy eliminated, gadolinium compounds are expected to provide ideal examples of Heisenberg spin systems, and the large ($\sim$7 μ_B) local moment generally leads to conveniently high ordering temperatures. However, as is common in many other areas, removing a dominant effect only makes other contributions more significant, and gadolinium compounds exhibit a rich variety of magnetic behaviour that derives in some cases from weaker effects (dipole–dipole interactions and intra-shell spin–orbit coupling can both lead to significant anisotropy) and in other cases from the crystal symmetry (geometrical frustration). As a result, gadolinium compounds are widely used to study the effects of dipole-driven anisotropy (Rotter *et al.*, 2003),

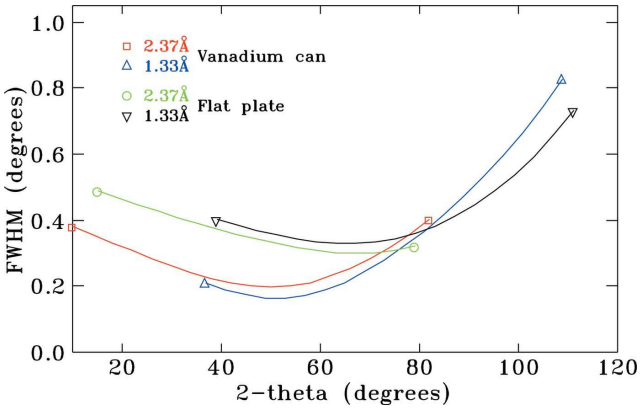

Figure 1
Peak resolution function derived from Rietveld fit to NIST Silicon 640*c* and Y_2O_3 on the C2 neutron powder diffractometer when packed in a standard vanadium sample holder (4.8 mm internal diameter) and a single-crystal silicon flat-plate sample holder oriented perpendicular to the beam. Ranges match the detector bank positions for data collection of 2θ = 5–85° for 2.37 Å and 2θ = 35–115° for 1.33 Å, which efficiently and effectively covers the range of Q (Bieringer, 2006; Potter *et al.*, 2007).

geometrically frustrated spin liquids and ices (Stewart *et al.*, 2004; Wills *et al.*, 2006; Mirebeau *et al.*, 2006) and entropy-driven ordering (Nakamura *et al.*, 1999). They also form the basis of a technologically important class of new materials that exhibit the giant magnetocaloric (GMC) effect (Pecharsky & Gschneidner, 1997; Gschneidner *et al.*, 2005).

The absorption cross section of gadolinium is strongly energy dependent (Goldberg *et al.*, 1966), and it was recognized in the late 1960s that by using higher energy (shorter wavelength) neutrons derived from either a thermal source (Cable & Wollan, 1968) or a spallation source (Ishikawa *et al.*, 1974) the absorption cross section could be reduced to a quite workable value of a few hundred barns. This approach is quite popular and dedicated instruments exist, exploiting hot sources at reactors [D4 at ILL (Fischer *et al.*, 2000), 7C2 at LLB (Forsythe, 1983), HEiDi at FRM-II (Meven *et al.*, 2007)] or time-of-flight instruments at spallation sources [KENS (Kuwahara *et al.*, 2002)]. The wavelengths used at the hot sources (0.58 Å at LLB; 0.47 Å at ILL) drive the scattering signal down to quite small angles in 2θ, leading to reduced resolution and problems with line overlap. This is especially problematic for magnetic diffraction signals, which tend to be concentrated in the low-angle range both because of the details of the magnetic structure (cell doubling *etc.*) and also because of the form factor for magnetic scattering (this latter problem is more marked in the rare earths). While time-of-flight techniques do not suffer as much from the loss of resolution, the strong energy dependence for both the absorption and scattering cross sections for elements like gadolinium (Goldberg *et al.*, 1966) greatly complicates the analysis. Furthermore, even with the reduced cross section, absorption is still significant, so samples are often limited in size and are typically contained in annular holders made from low-background materials such as aluminium, with the sample occupying a 1 mm thick annulus between two thin-walled tubes.

A second strategy derives from the recognition that the problem with natural gadolinium arises almost entirely from the 15% of ^{155}Gd and 16% of ^{157}Gd that are present. If isotopically separated material is used in the preparation of the samples, then the absorption problem can be eliminated. Popular choices are ^{160}Gd and, to a lesser extent, ^{158}Gd. This solution is not perfect as it involves trading the problem of almost total absorption for that of making samples from relatively small amounts of starting material. The cost of the separated isotopes (USD10–20 mg^{-1}) means that preparation typically starts with only 200–300 mg of gadolinium metal and final sample sizes are of order 500 mg. As a result, such studies are confined to only the most promising of materials.

The restricted availability of hot-source diffraction instruments greatly limits the first approach, while the costs and significant risks associated with making samples based on ^{160}Gd limit application of the second. An examination of the extensive neutron-based literature on magnetic rare earth compounds reveals that there is a third, and currently dominant, approach to the problem of working with gadolinium compounds when studying a series of materials: skip over it. The numerous examples of compound series where the magnetic structures of all but the gadolinium member have been determined reveal that there is a genuine need for a simpler, more routine, solution to the problem.

3. Neutron scattering cross sections and absorption lengths for Sm, Gd and Eu

Over the range of thermal neutron wavelengths used for reactor-based neutron beam experiments, most elements are normally treated as having constant scattering cross sections and absorption lengths. Values tabulated at a wavelength of 1.798 Å (E = 0.0253 eV), by Sears (1992) or Rauch & Waschkowski (2003), are typically used. However, the heavily absorbing elements such as Sm, Gd and Eu are subject to resonances, which result in the scattering lengths and absorption at thermal neutron wavelengths being both energy dependent and complex (Larson & Von Dreele, 2004, pp. 123–124). For experiments to understand magnetic crystal structures, this is of considerable consequence, as magnetic moments derived from a Rietveld analysis of the observed diffraction pattern are affected by the choice of both the nuclear scattering lengths and the absorption correction applied to the data.

Our calculations of optimum sample thicknesses used the 'default' cross-section values of Rauch & Waschkowski (2003) for planning purposes. However, more complete data on scattering cross-section data for these elements as a function of wavelength are provided by Lynn & Seeger (1990), while absorption cross-section data are provided by Goldberg *et al.* (1966). A more recent summary of tabulated cross-section data for pure isotopes may be found in the monograph by Mughabghab (2006).

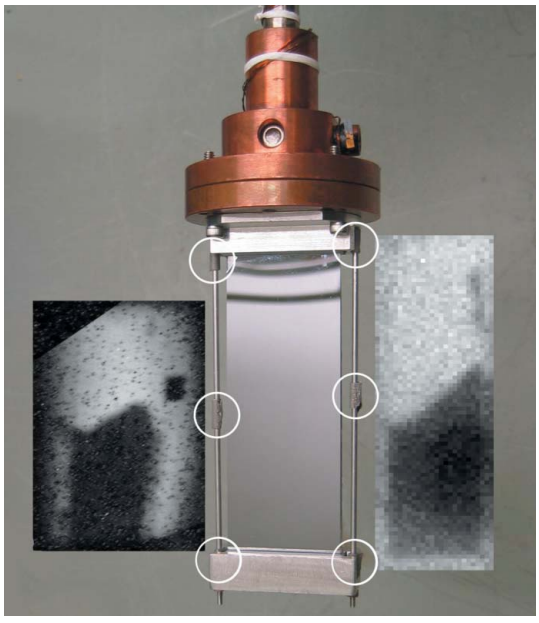

Figure 2
Photograph of the silicon flat-plate holder with (left) neutron video camera image and (right) γ-ray density image of the $Sm_3Ag_4Sn_4$ sample, showing clear evidence of settling. The neutron image was taken with the sample normal at 30° to the beam so that the entire holder was illuminated. Dead pixels have been removed and the image has been stretched horizontally to match the optical image. The six cadmium marker tags mounted on the vertical supports are circled and one is visible as a dark shadow to the right of the sample in the neutron camera image. The γ-ray density image was obtained off-line with a 1 mm step size at 122 keV and covers the whole area of the sample.

4. Initial testing with $Sm_3Ag_4Sn_4$: peak resolution function and settling of the sample

In order to obtain a *GSAS* instrument parameter file (Larson & Von Dreele, 2004) appropriate for our flat-plate geometry, equal masses of NIST silicon 640*c* and annealed cubic Y_2O_3 were mixed and loaded into a flat-plate holder using strips of 150 µm thick vanadium foil as a gasket/spacer. The Y_2O_3 (Alfar–Aesar, 99.99%, annealed in air at 1473 K for 2 d) was added to the silicon to provide extra reflections for modelling the zero offset at 2.37 Å, since silicon gives only three diffraction peaks in the available 80° 2θ range and thus provides insufficient information for a refinement of the instrumental parameters affecting peak position (wavelength and zero offset). The plate was orientated perpendicular to the beam. The refined peak widths are shown in Fig. 1 and it is clear that there is some loss of resolution associated with this large-area scattering geometry. The effect of the flat plate is to have a minimum full width at half-maximum (FWHM) of 0.328° at around 2θ = 67° at 2.37 Å, whereas a standard 4.8 mm inside diameter vanadium sample holder yields a minimum width of 0.187° at 2θ = 53° at 2.37 Å.

Our first test of the large-area flat-plate holder with a metallic sample used $Sm_3Ag_4Sn_4$. Estimates of absorption for this material yielded an expected $1/e$ thickness of 125 mg cm^{-2} or about 140 µm, so we used strips of 150 µm thick vanadium foil around the four edges of the silicon plate to form a gasket

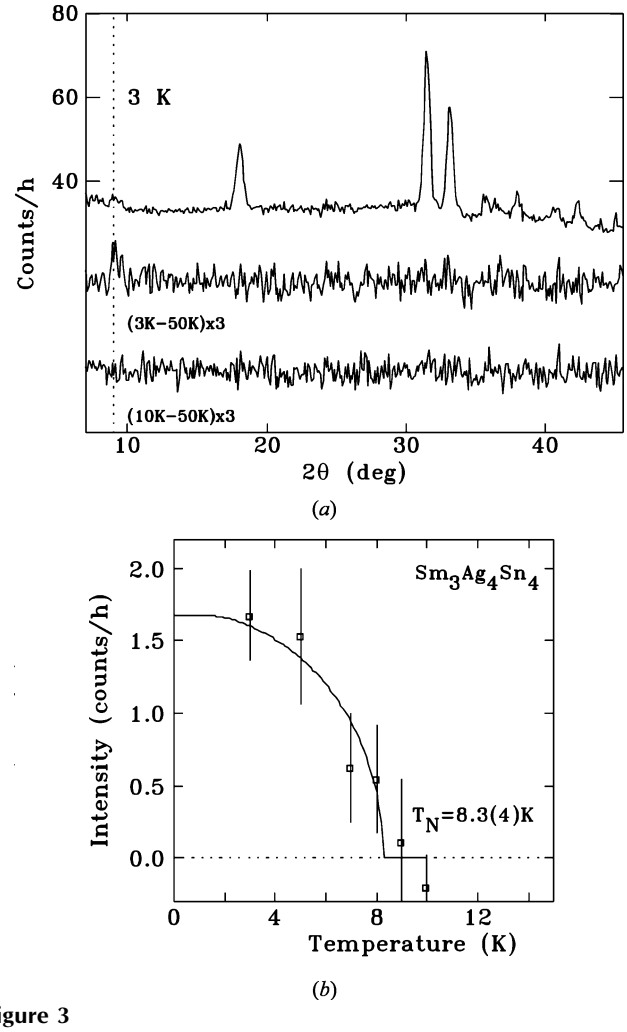

Figure 3
(*a*) Raw neutron diffraction data of $Sm_3Ag_4Sn_4$ collected at 3 K, showing the small 100 magnetic peak at $2\theta \simeq 9°$, with ×3 difference plots accentuating the magnetic peak. The neutron diffraction data are only sensitive enough to detect magnetic peaks from the lowest temperature magnetic phase. (*b*) The temperature dependence of the 100 magnetic peak fitted to a J = 4 Brillouin function and yielding a transition temperature of 8.3 (4) K.

that would define the space for the sample to occupy. The sample was loaded as before by forming a slurry with ethanol which could then be spread uniformly into the gasketed volume. After drying overnight, the cover plate was installed and clamped in place. The total sample mass used was 1.57 g, giving a final area density of 80 mg cm^{-2}.

A neutron video camera was used to align the sample in the beam, and during this process we found that the powdered $Sm_3Ag_4Sn_4$ sample had settled between the two silicon plates and only occupied the lower half of the sample holder (Fig. 2). An off-line density measurement using 122 keV γ-rays confirmed this settling. The change in sample distribution was surprising, as previous runs using Eu_2BaNiO_5 had not shown any evidence of movement during the measurement. Subsequent examination of the two materials revealed that the Eu_2BaNiO_5 had a clear tendency to 'cake' or stick to itself, even when nominally dry, while the $Sm_3Ag_4Sn_4$ sample formed a free-flowing powder once the solvent evaporated.

The settled $Sm_3Ag_4Sn_4$ sample had an approximate area density of 160 mg cm^{-2}, somewhat higher than originally intended. However, with the slits set to illuminate only the filled region of the holder, we found that the signal was strong enough to be useful and the neutron data still turned out to be adequate for analysis. Solutions to the settling problem will be discussed below.

4.1. Magnetic diffraction of the highly absorbing samarium phase $Sm_3Ag_4Sn_4$

Neutron diffraction data collected at 50 K were of sufficient quality to permit a full Rietveld refinement using *GSAS* (Larson & Von Dreele, 2004) and *EXPGUI* (Toby, 2001) and were consistent with data from Cu $K\alpha$ X-ray diffraction. However, it is the low-temperature magnetic data that formed the intended focus of our work. Fig. 3(*a*) shows the pattern obtained at 3 K, with the 50 K data subtracted to emphasize the magnetic signal at $2\theta = 9°$. The single magnetic peak seen at 3 K was identified as being due to the 100 reflection and, while it is extremely weak, we were able to follow its temperature dependence, and a fit to a $J = 4$ Brillouin function, appropriate for Sm, yields a transition temperature of 8.3 (4) K (Fig. 3*b*), consistent with other measurements (Voyer, Ryan, Cadogan *et al.*, 2007). Evaluation of the allowed magnetic space groups enabled us to identify the most likely magnetic structure as being I_Pmmm', which only allows ordering on one of the two samarium sites (the 4*e*), and analysis of the peak intensity yields a moment of 0.47 (10) μ_B for the Sm 4*e* site at 3 K.

5. Neutron powder diffraction of gadolinium compounds

Encouraged by our success with $Sm_3Ag_4Sn_4$, we considered the possibility of repeating the experiment using the gadolinium member of the series. The conventional value for the absorption cross section of natural gadolinium is 49700 (125) b, tabulated at a wavelength of 1.80 Å (Rauch & Waschkowski, 2003). However, it is quite strongly energy dependent and by 1.33 Å it is down to ∼35000 b (Goldberg *et al.*, 1966). Our interest in magnetic ordering and the expectation that many of the magnetic peaks will occur at low Q make the shorter wavelength choice unsuitable and we therefore worked at 2.37 Å, where the absorption cross section is estimated to be ∼60000 b (Goldberg *et al.*, 1966). Evaluation of the neutron absorption for $Gd_3Ag_4Sn_4$ using an absorption cross section of 60000 b for the gadolinium yields a 1/*e* thickness of about 14 µm or 12 mg cm^{-2} for a total sample mass of 230 mg. This might seem small, but examination of the literature reveals that most of the gadolinium samples that have been prepared using ^{160}Gd have masses of 500–600 mg, this value being limited by the significant cost of the isotope. While we would be losing a factor of two in total scattering by using the smaller sample, and a further factor of *e* for absorption, we expect to more than compensate by using the full area of the incident beam and so making our total incident flux much higher. Furthermore, the expected 7 μ_B moment on the gadolinium should yield nearly 200 times more magnetic scattering than the 0.5 μ_B samarium moment that we were able to detect in $Sm_3Ag_4Sn_4$, so the magnetic signal should be much clearer.

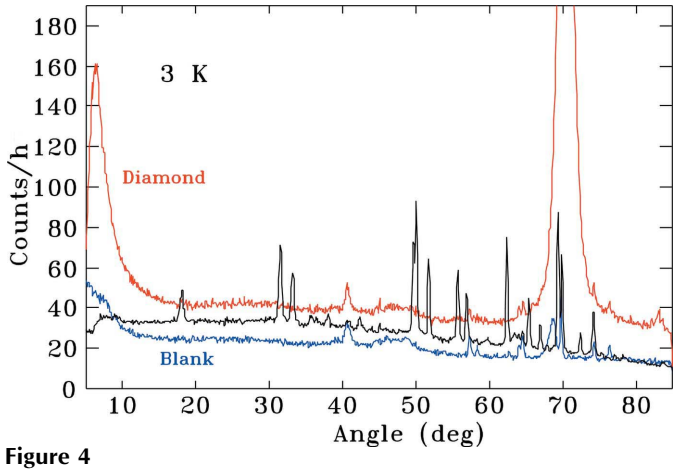

Figure 4
Neutron powder diffraction data collected at a temperature of 3 K and plotted as counts h^{-1} for 620 mg of diamond powder in a single-crystal silicon flat-plate sample (upper curve), 1.57 g of $Sm_3Ag_4Sn_4$ in the same holder (middle curve) and just the single-crystal silicon plates (lowest curve, 'Blank'). It is clear that the background from the diamond powder is excessive below $2\theta = 15°$. The edge wires of the detector are deliberately shielded to limit stray neutrons entering the sides of the detector and scattering onto other detector wires.

Working with natural-abundance materials brings several advantages, starting with cost. We are able to make much larger samples so that all of our measurements (X-ray diffraction, magnetometry, Mössbauer spectroscopy and neutron diffraction) can be made on a single batch. We do not have to develop separate techniques for the synthesis of small samples or worry that the material prepared from the isotope is not identical to the larger syntheses with natural materials. Our final operating masses are comparable with those used with isotopic syntheses, so using compounds synthesized using natural-abundance elements and running them in the silicon flat-plate sample holder should be experimentally competitive with isotopic enrichment.

Our experience with the settling of the $Sm_3Ag_4Sn_4$ sample led us to expect more severe problems with mounting a sample that will be about 10% of the thickness. We therefore investigated two possible solutions: (i) diluting the sample with a clean weakly scattering material so that the total thickness could be made more manageable; (ii) immobilizing the sample with some form of glue.

5.1. Crystalline diluent powder: synthetic diamond

Synthetic diamond powder is a popular diluent for X-ray diffraction work as its low Z leads to weak scattering and the synthetic powders are extremely clean. The structure also yields a small number of easily identified peaks. We explored the use of diamond as a highly crystalline low-absorbance diluent in our flat-plate holder, but the low-angle background

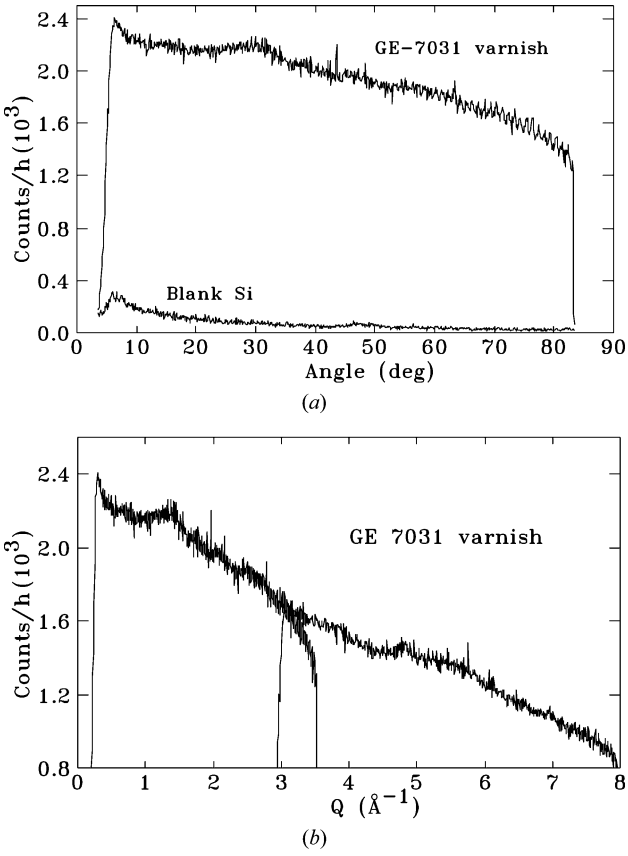

Figure 5
Neutron powder diffraction data of 2 g of GE-7031 varnish mounted on a silicon flat-plate sample holder: (*a*) at 2.37 Å and compared with the blank silicon sample holder; (*b*) as a function of Q using 2.37 and 1.33 Å data, showing the effect of hydrogen within the GE varnish and also the increasing absorption in the 2.37 Å data near $Q = 3$ Å^{-1} as the scattered beam passes almost parallel to the plate surface. The saw-tooth form of the background is due to effects of the oscillating collimator on the C2 neutron powder diffractometer. The edge wires of the detector are deliberately shielded to limit stray neutrons entering the sides of the detector and scattering onto other detector wires.

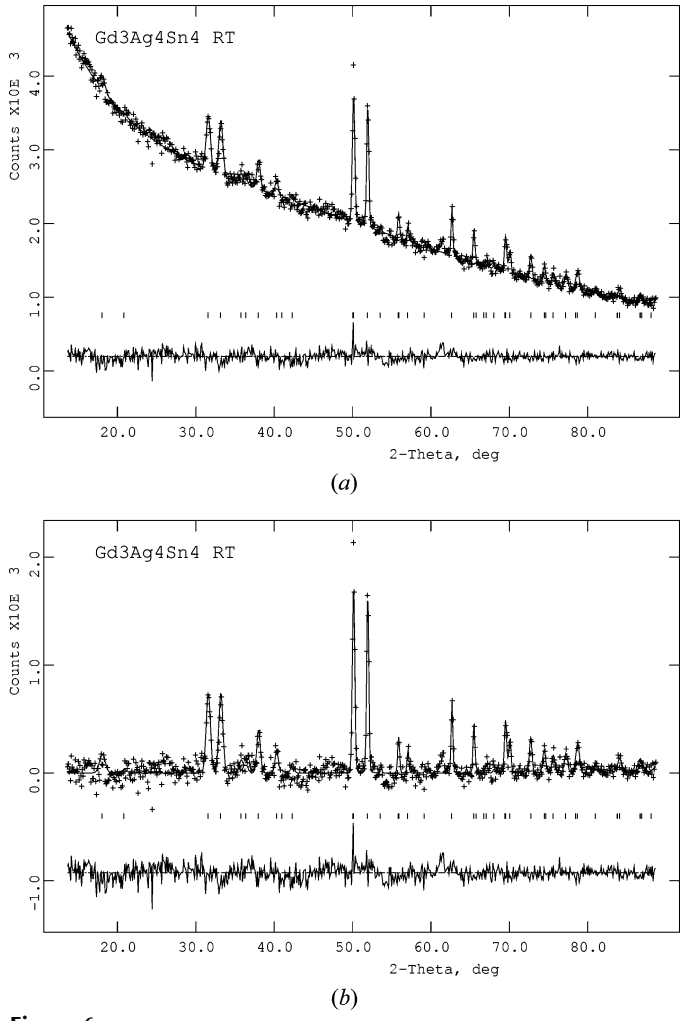

Figure 6
Profile refinement of the neutron powder diffraction pattern obtained *via GSAS* using the published nuclear structure of $Gd_3Ag_4Sn_4$ and only allowing the lattice parameters to vary. The neutron powder diffraction data were collected in air at room temperature over 51 h at 2.37 Å with a ~20 µm thick 300 mg layer of $Gd_3Ag_4Sn_4$. (*a*) Raw data. (*b*) Data with the background subtracted to emphasize the fit.

was found to be excessive (Fig. 4). This was unacceptable as it occurs precisely in the range where magnetic diffraction from the sample should be most pronounced. It is likely that any diluent will cause similar background contributions simply because there will always need to be much more of the diluent than the sample in order to bulk up the total volume enough to fill the holder.

5.2. Immobilization using highly dilute GE-7031 varnish

GE-7031 varnish is a ubiquitous material in low-temperature research laboratories. It is readily available and has been used routinely on systems that are cooled to mK temperatures. It was therefore our first choice for a glue to immobilize the sample. Two evaluation experiments were performed: (i) to determine how little GE-7031 varnish was needed to immobilize the sample safely; (ii) to measure the scattering by GE-7031 varnish to determine the expected additional contribution to the background.

Several diluted batches of GE-7031 varnish were prepared by mixing the starting varnish with the standard 50:50 (*v*/*v*) toluene–methanol solvent to form 10%, 5% and 1% solutions (by weight) and using an ultrasonic bath to improve uniformity. Approximately 0.2 ml of each solution was added to 300 mg of powdered $Gd_3Cu_4Sn_4$ and the slurry was loaded into a flat-plate sample holder and allowed to dry overnight. Each sample was checked for mechanical hold and then cycled twice between 77 K and room temperature to confirm adhesion. Even the 1% solution provided adequate performance and so this was adopted as our standard method. We estimate that at this concentration we add approximately 2 mg of the starting varnish to the sample.

To assess the potential background contribution from the varnish, we prepared a reference sample using 2 g of undiluted GE-7031 varnish mounted on a silicon plate. The diffraction pattern (Fig. 5) shows no sharp features and a count rate of ~2100 counts h^{-1} in the low-angle region of particular

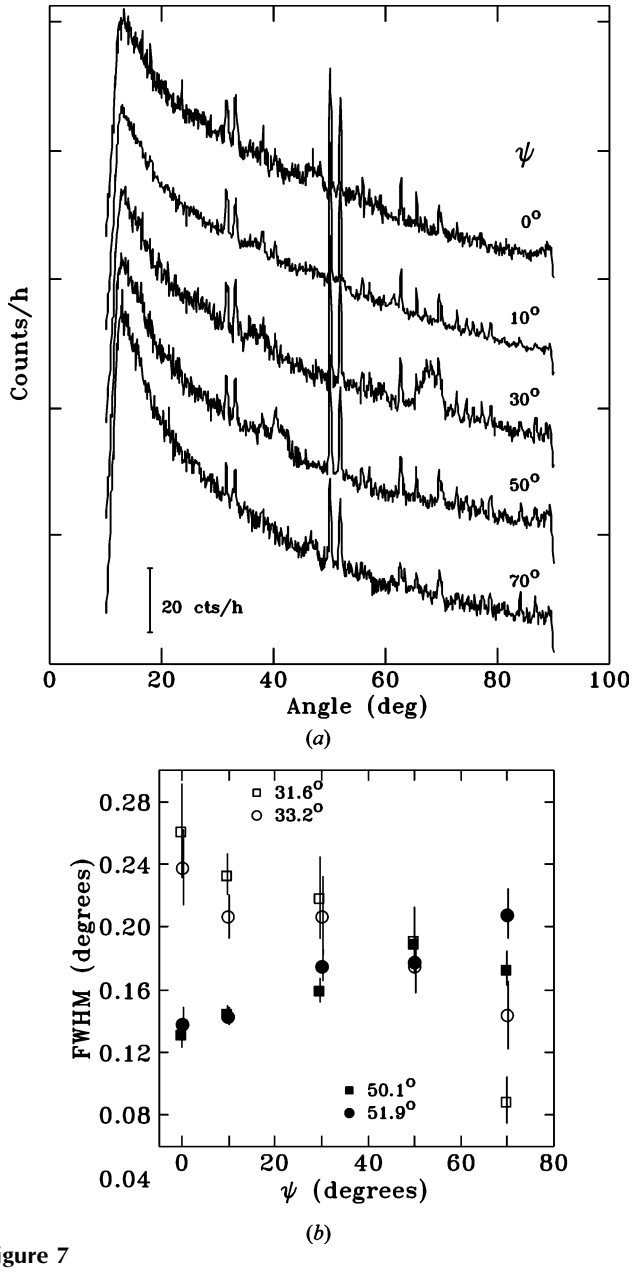

Figure 7
Effect of rotation of the silicon plate, showing the change in the peak width of $Gd_3Ag_4Sn_4$ at room temperature ($\psi = 90^\circ$ corresponds to the plate surface being parallel to the neutron beam). (*a*) Raw neutron diffraction data with 30 counts h^{-1} offset. (*b*) Widths (FWHM) of several peaks as a function of silicon plate angle. The broad structure evident in the $\psi = 30^\circ$ pattern for $60 < 2\theta < 70^\circ$ is due to inelastic scattering by phonons in the silicon plates. The edge wires of the detector are deliberately shielded to limit stray neutrons entering the sides of the detector and scattering onto other detector wires.

concern to us. The fall-off in signal evident at high Q is typical of a proton-rich material. Examination of the overlap region between the two data sets in Fig. 5(*b*) near $Q = 3$ Å^{-1} reveals the effects of absorption as the scattered beam passes almost parallel to the plate surface. The 1% varnish solution used to immobilize the sample adds about 2 mg of varnish to the sample, *i.e.* 0.1% of the 2 g (initial wet weight) used in Fig. 5. Below $2\theta = 30^\circ$, where most of the magnetic scattering is expected to occur, we estimate that the additional background

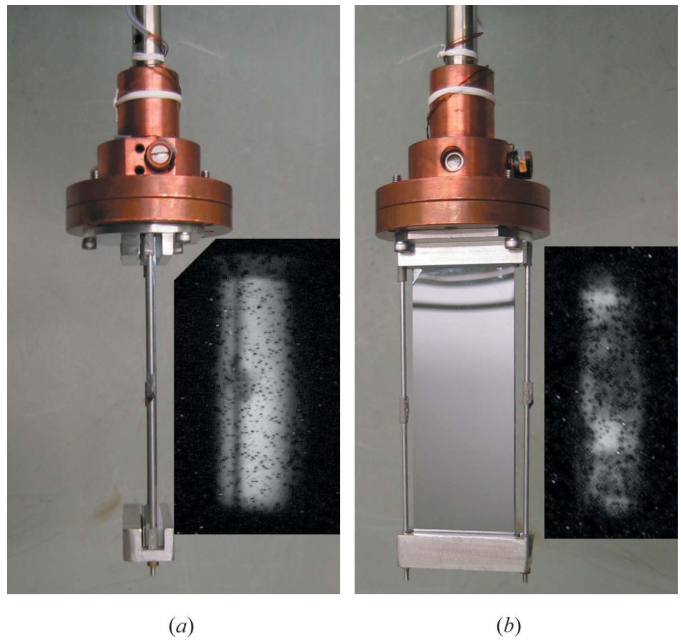

Figure 8
Photographs and corresponding neutron camera images of the silicon plates (30 × 90 × 0.7 mm each) sandwiching ∼20 µm thick $Gd_3Ag_4Sn_4$ powder bound by GE-7031 varnish, with a 150 µm vanadium gasket to stop the two plates touching, and with cadmium metal markers to help identify sample limits. (*a*) Plate parallel to the neutron beam, with the thin strip of $Gd_3Ag_4Sn_4$ and the two cadmium markers evident. (*b*) Plate perpendicular to the neutron beam, showing some inhomogeneity in sample thickness. Neutron camera images have been processed to subtract dead pixels. While clamping the bottom without using the aluminium struts permits operation with a very wide neutron beam or at any sample orientation, the struts prevent the plate falling out if the clamping fails and they reduce the need to over-tighten the clamps and risk breaking the plates.

from the GE-7031 varnish will amount to about 2 counts h^{-1}, or less than 3% of the background contributed by the silicon plates used as a substrate for the sample.

An initial room-temperature test run using 300 mg of $Gd_3Ag_4Sn_4$ fixed to a silicon plate with a 1% solution of GE-7031 varnish was performed to confirm feasibility. This resulted in ∼50 counts h^{-1} on the maximum peak to give Rietveld refinement quality data in 51 h (Fig. 6). As expected, there was no background from the GE-7031 varnish used to immobilize the sample. The observed intensities in the neutron diffraction pattern are a good match with the intensities calculated from the published structure (Salamakha *et al.*, 1996). Our refined lattice parameters are $a = 15.222$ (5), $b = 7.3075$ (25) and $c = 4.5669$ (15) Å, compared with the literature values of $a = 15.211$ (6), $b = 7.308$ (3) and $c = 4.567$ (2) Å derived from Cu $K\alpha$ X-ray diffraction data (Mazzone *et al.*, 2005).

5.3. Effect of orientation of sample plate with respect to the beam

Rather than use a non-absorbing standard material, we preferred to use the real $Gd_3Ag_4Sn_4$ sample to confirm the actual effects of orientation on a highly absorbing sample, including scatter from the silicon sample plate. This evaluation

was performed using the sample mounted on a single silicon plate with no aluminium mounting posts, so that the plate could be rotated to extreme angles. Differing scatter from the silicon plate is evident as a function of plate angle (Fig. 7*a*) and is dominated by inelastic scatter from the silicon [confirmed in our earlier paper by cooling the sample (Potter *et al.*, 2007)]. This means that some optimization for location and strength of background can be achieved. The change in peak width is also plotted (Fig. 7*b*) and this variation reflects the angle subtended at the detector by the large flat-plate sample. The low-angle peaks are much broader with the plate perpendicular to the beam, but not so broad as to preclude this orientation being used to optimize background scatter. Some improvement in line width is possible by rotating the sample away from $\psi = 0°$ and this could be useful where increased peak to background ratios are essential to detect a weak magnetic peak, as long as increased sample absorption does not counter the benefits.

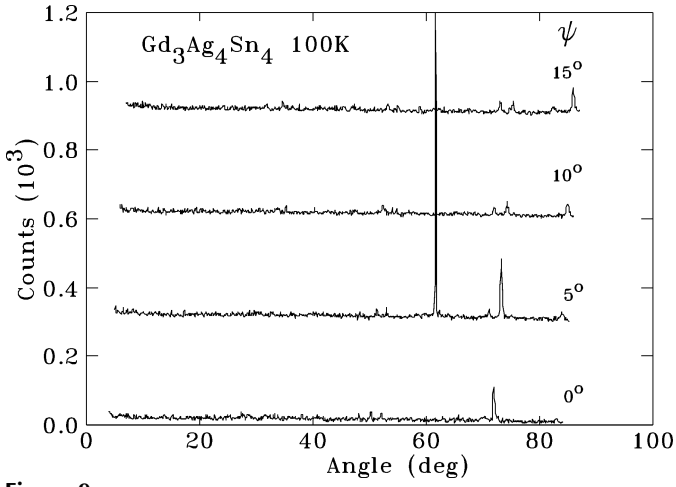

Figure 9
When performing the actual magnetism experiment, it is essential to check for potential spurious peaks by rotating the sample holder, and to select an orientation that yields the minimum interfering scatter. The peaks are due to non-Bragg inelastic scatter.

6. Magnetic data at 2.37 Å for $Gd_3Ag_4Sn_4$

6.1. Mounting and orienting the sample for minimum background

$Gd_3Ag_4Sn_4$ (300 mg) was mounted on a large-area flat-plate sample holder using a 1% solution of GE-7031 varnish to immobilize the sample. The methodology for setting the neutron beam illumination onto the sample was as before (Potter *et al.*, 2007) and was guided by the use of a home-made neutron video camera mounted in the beam. Fig. 8 shows the alignment and sample checking within the closed-cycle refrigerator using a home-made neutron video camera, as matched with the orientation of the sample holder when photographed outside the closed-cycle refrigerator. It is clear in Fig. 8(*b*) that there is some non-uniformity in the sample distribution. However, there is no evidence of settling.

While the single-crystal silicon plates yield a remarkably low background, they have a mass that is 30–40 times that of the sample and they do scatter neutrons. With low count rates, even small amounts of accidental scatter from the sample holder or spurious peaks can have a significant effect on the pattern. Thus, prior to taking the sample below the magnetic transition, it can be important to know the expected nuclear diffraction pattern, and to use this information to check for spurious peaks as a function of angle close to the desired plate setting. Fig. 9 shows a range of spurious peaks from 30 min scans at a variety of angular settings of the silicon plate.

6.2. Observation of magnetic scattering for $Gd_3Ag_4Sn_4$

Fig. 10(*a*) shows the resulting raw neutron powder diffraction data for $Gd_3Ag_4Sn_4$, displaying strong magnetic diffraction peaks between $2\theta = 8$ and 45°. Fig. 10(*b*) shows the intensity of several of the major magnetic reflections as a function of temperature. It is immediately clear that a magnetic signal can be observed in $Gd_3Ag_4Sn_4$ using the flat-plate holder. The two magnetic transitions at 8 and 28 K, previously inferred from ^{119}Sn Mössbauer measurements, are

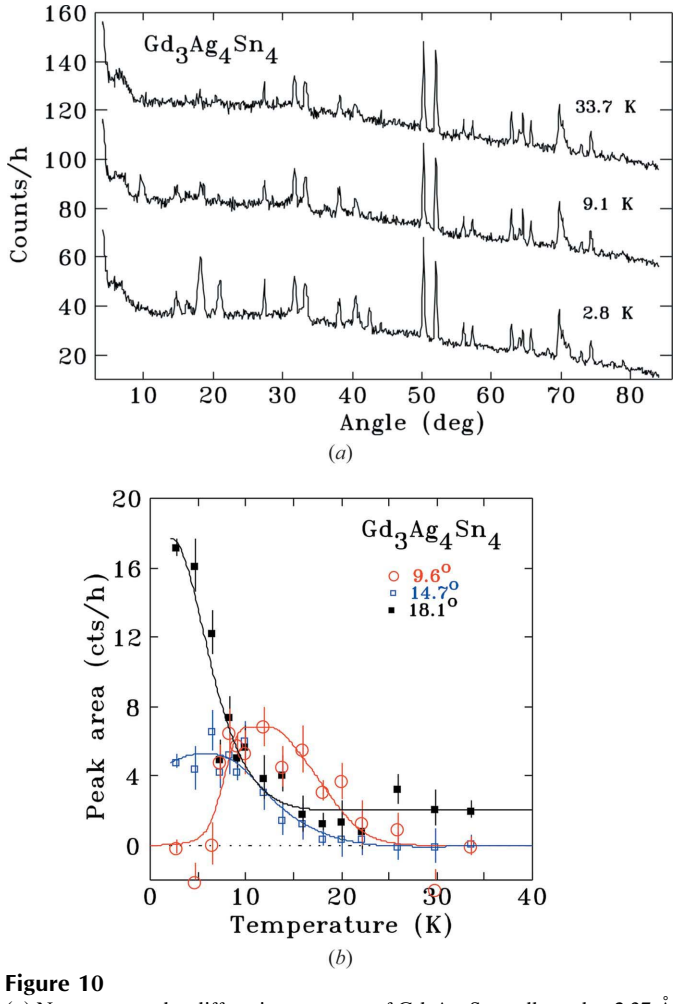

Figure 10
(*a*) Neutron powder diffraction patterns of $Gd_3Ag_4Sn_4$ collected at 2.37 Å and at temperatures of 2.8, 9.1 and 33.7 K, showing two magnetic phases. (*b*) Temperature-dependence plots following the main magnetic peaks as a function of temperature. A group of strong magnetic peaks is visible in the 2.8 K data between $2\theta = 15°$ and $2\theta = 45°$. A change in magnetic structure above 9 K is signalled by the appearance of a new magnetic peak around $2\theta = 9°$.

also fully confirmed (Voyer, Ryan, Napoletano & Riani, 2007). Finally, the evolution of the magnetic reflection at $2\theta = 9.6^\circ$ is consistent with the transition at 8 K being a 90° spin reorientation, as suggested earlier (Voyer, Ryan, Napoletano & Riani, 2007).

7. Conclusions

We have demonstrated that it is possible to obtain useful neutron powder diffraction data at conventional thermal wavelengths (2.37 Å) for compounds of samarium and gadolinium without resorting to isotopically separated materials. The flat-plate single-crystal silicon sample holder can be used on conventional thermal beamlines. Counter-intuitively, experiments on gadolinium samples can require less beam time than those on less absorbing europium and samarium compounds, due to the strong magnetic scattering by the large gadolinium moments. By contrast, europium and samarium compounds have much smaller magnetic moments and it can take longer counting times to observe, or fail to observe, magnetic peaks above the background noise.

The low-temperature portion of the $Gd_3Ag_4Sn_4$ experiment took 8 d of neutron beam time on the C2 diffractometer at Chalk River using the standard beamline configuration described by Potter *et al.* (2007). However, the combination of higher incident flux and large-area detectors available at some other facilities could reduce the required counting times by as much as a factor of 100 (Hunter, 2000; Hewat, 2006; Liss *et al.*, 2006; Studer *et al.*, 2006). The above examples show that even with gadolinium, the most severely neutron absorbing element in the Periodic Table, the flat-plate single-crystal silicon sample holder, combined with dilute GE-7031 varnish as a binder, allows for a moderately routine experiment to collect data for the solution and refinement of the magnetic structures of these highly absorbing phases.

We are grateful to the McGill–MIAM Micromachining Facility for cutting the silicon wafers; Chris Voyer (McGill) for preparing the Eu_2BaNiO_5 and $Gd_3Cu_4Sn_4$ samples used during the initial development of the flat-plate sample holder, and for the Rietveld refinement of the room-temperature diffraction pattern of $Gd_3Ag_4Sn_4$; J. M. Cadogan (University of Manitoba) for many useful discussions; Larry McEwan of CNBC for machining; and Raymond Sammon, Travis Dodd and Dave Dean of CNBC for setup of the closed-cycle refrigeration systems. The $Sm_3Ag_4Sn_4$ and $Gd_3Ag_4Sn_4$ samples were prepared by P. Riani (University of Genova). Stephen Sabbaghian and Marcelo Wu (McGill) provided the γ-ray density map used in Fig. 2. We thank the editor, Professor John R. Helliwell, for his guidance, and the two referees for their helpful input.

References

Bieringer, M. (2006). Personal communication.
Cable, J. W. & Wollan, E. O. (1968). *Phys. Rev.* **165**, 733–734.
Fischer, H. E., Palleau, P. & Feltin, D. (2000). *Physica B*, **276–278**, 93–94.
Forsythe, B. (1983). In *Position Sensitive Detection of Thermal Neutrons*, edited by P. Convert. London: Academic Press.
Goldberg, M. D., Mughabghab, S. F., Purohit, S. N., Magurno, B. A. & May, V. M. (1966). *Neutron Cross Sections Volume IIC, Z = 61 to 87*, BNL 325, 2nd ed., Suppl. No. 2 (Physics – TID-4500). Brookhaven National Laboratory, USA.
Gschneidner, K. A., Pecharsky, V. K. & Tsokol, A. O. (2005). *Rep. Prog. Phys.* **68**, 1479–1539.
Hewat, A. W. (2006). *Physica B Condens. Matter*, **385–386**, 979–984.
Hunter, B. (2000). Editor. *Report on Neutron Powder Diffraction for the Australian Replacement Research Reactor*, pp. 24–25. Australian Nuclear Science and Technology Organization (ANSTO), Lucas Heights, Australia.
Ishikawa, Y., Watanabe, N., Tajima, K. & Sekine, H. (1974). *Phys. Lett. A*, **48**, 159–160.
Kuwahara, K., Sugiyama, S., Iwasa, K., Kohgi, M., Nakamura, M., Inamura, Y., Arai, M. & Kunii, S. (2002). *Appl. Phys. A*, **74**, S302–S304.
Larson, A. C. & Von Dreele, R. B. (2004). *GSAS*. Report LAUR 86-748. Los Alamos National Laboratory, Los Alamos, New Mexico, USA.
Liss, K.-D., Hunter, B., Hagen, M., Noakes, T. & Kennedy, S. (2006). *Physica B Condens. Matter*, **385–386**, 1010–1012.
Lynn, J. E. & Seeger, P. A. (1990). *At. Data Nucl. Data Tables*, **44**, 191–207.
Mazzone, D., Riani, P., Napoletano, M. & Canepa, F. (2005). *J. Alloys Compd.* **387**, 15–19.
Meven, M., Hutanu, V. & Heger, G. (2007). *Neutron News*, **18**, 19–21.
Mirebeau, I., Apetrei, A., Goncharenko, I., Andreica, D., Bonville, P., Sanchez, P., Amato, A., Suard, E., Crichton, W. A., Forget, A. & Colson, D. (2006). *Phys. Rev. B*, **74**, 174414.
Mughabghab, S. F. (2006). *Atlas of Neutron Resonances*, 5th ed. Amsterdam: Elsevier Science.
Nakamura, H., Kim, N., Shiga, M., Kmiec, R., Tomala, K., Ressouche, E., Sanchez, J. P. & Malaman, B. (1999). *J. Phys. Condens. Matter*, **11**, 1095–1104.
Pecharsky, V. K. & Gschneidner, K. A. (1997). *Phys. Rev. Lett.* **78**, 4494–4497.
Potter, M., Fritzsche, H., Ryan, D. H. & Cranswick, L. M. D. (2007). *J. Appl. Cryst.* **40**, 489–495.
Rauch, H. & Waschkowski, W. (2003). *Neutron Data Booklet*, edited by A.-J. Dianoux & G. Lander. Philadelphia: Old City Publishing (OCP) Science.
Rotter, M., Loewenhaupt, M., Doerr, M., Lindbaum, A., Sassik, H., Ziebeck, K. & Beuneu, B. (2003). *Phys. Rev. B*, **68**, 144418.
Salamakha, P. S., Zaplatyndky, O. V., Sologub, O. L. & Bodak, O. I. (1996). *Pol. J. Chem.* **70**, 158.
Sears, V. F. (1992). *Neutron News*, **3**, 26–37.
Stewart, J. R., Ehlers, G., Wills, A. S., Bramwell, S. T. & Gardner, J. S. (2004). *J. Phys. Condens. Matter*, **16**, L321–L326.
Studer, A. J., Hagen, M. E. & Noakes, T. J. (2006). *Physica B Condens. Matter*, **385–386**, 1013–1015.
Toby, B. H. (2001). *J. Appl. Cryst.* **34**, 210–213.
Voyer, C. J., Ryan, D. H., Cadogan, J. M., Cranswick, L. M. D., Napoletano, M., Riani, P. & Canepa, F. (2007). *J. Phys. Condens. Matter*, **19**, 436205.
Voyer, C. J., Ryan, D. H., Napoletano, M. & Riani, P. (2007). *J. Phys. Condens. Matter*, **19**, 156209.
Wills, A. S., Zhitomirsky, M. E., Canals, B., Sanchez, J. P., Bonville, P., Dalmas de Réotier, P. & Yaouanc, A. (2006). *J. Phys. Condens. Matter*, **18**, L37–L42.